Series Balancing Capacitor (SBC) based DMPPT Scheme for string of PV Modules operating under non-uniform operating conditions

Neil Samaddar[1], V Gouri Prasant[2], Arpan Kumar Samanta[3], Moningi Srivalli[4], and Dipankar Debnath[5], *SMIEEE*[5]
Department of Electrical Engineering, Indian Institute of Technology Kharagpur, Kharagpur, West Bengal 721302, India
[1]neil.samaddar@outlook.com,[2]prasant.vgp@gmail.com, [3]arpansamanta0098@gmail.com,
[4]m.srivalli@kgpian.iitkgp.ac.in,[5]ddebnath@ee.iitkgp.ac.in.

***Abstract*—In a Photovoltaic (PV) system, modules are connected in series and parallel combinations to achieve desired voltage and current ratings. However, a string of PV modules can have a vastly reduced energy output during non-uniform operating conditions. This paper introduces a new Distributed MPPT (DMPPT) architecture using a Balancing Capacitor connected in series with a string of PV modules, having MPP and non-MPP functionality (where the system will output a desired amount of power). Each PV module in this scheme has a partial power processing (PPP) DC-DC converter connected across them to allow them to operate at a desired voltage depending on the system requirements. In comparison to other DMPPT schemes, this architecture can easily be integrated with a DC grid without the need of additional power electronic stages, at the same time allowing the PV modules to operate at their maximum power points (MPPs) if the system demands it. This scheme has been validated using detailed simulations and results are presented to verify the proposed architecture.**

***Index Terms*—Series Balancing Capacitor (SBC), Partial Power Processing (PPP), DC Bus Voltage, Building Integrated PV (BIPV), Distributed Maximum Power Point Tracking (DMPPT).**

I. Introduction

In the current scenario, large PV plants represent the majority of the installed PV capacity. However, PV systems present an unique opportunity to integrate it with the urban infrastructure like BIPV (Building Integrated PV), but PV modules in such systems suffer from the greatly different operating conditions due to varying inclination to sunlight, partial or complete shadows, dust, soiling, etc. This causes a significant portion of the available power to be lost. Hence, to maximize the power extraction from the PV modules they should be operated at their maximum power points. This can be achieved in 2 ways - either by using a central converter across the entire string or using a distributed architecture [1][2][3] where the string is divided into smaller elements and converters are connected across those elements. However, as stated in [4], using distributed architecture can give up to a 25% higher output power when PV modules experience different operating conditions, which is very common in urban environments. In addition to this, DMPPT topologies have a higher system reliability, since a malfunction of any module converter will not compromise the entire string, although the overall power output may get reduced [5].

The distributed architecture topologies for mismatched PV modules connected in series reported in the literature include:

In [6], [7], and [8], distributed architectures featuring partial power processing (PPP) converters connected across individual PV modules have been illustrated. The scheme presented in [7] suggests a minimized current sensor requirement, while reference [8] goes even further by proposing a reduced voltage sensor count. Three module level voltage equalization DMPPT schemes have been presented in [9] - series resonant voltage multiplier, Flyback based PV to IP (Isolated Port) and Flyback based PV to Bus. However, in these architectures, the string voltage is the summation of the PV voltages, as a result the string voltage varies as the operating point of the PV modules change according to the operating conditions of the modules, which will make it difficult to integrate this system to a DC grid without the use of additional converters. Moreover, the input of the DC-DC converters is across the entire string voltage, as a result the switches would need to be of higher voltage rating, which would increase the cost of the switches. Additionally, if the voltage requirement exceeds 650V, which is the typical voltage requirement in most string level systems, IGBTs have to be used instead of MOSFETS. As a consequence, the DC-DC converters have to be operated at much lower switching frequency, causing the size of the transformer and filter elements to go up. In [10], [11] and [12], a submodule distributed topology is implemented where a single module is divided into n segments and PPP converters achieve MPP of each segment. In [11], additionally a series virtual port is connected with each submodule. The architecture shown in [13] is also a sub-module DMPPT architecture based on multi-port DC-DC converter with a reduced number of switches and current sensors. In these configurations, if a higher DC voltage is required, then the number of modules connected in series have to be increased which in turn would increase the number of power electronic converters to n times the number of modules. This makes the scalability of these architectures difficult, especially in systems where the string voltage requirement is much higher than the MPP voltage of one module. In [14], a segmented DPP architecture is adopted

where a string of PV modules is divided into n/m segments, where n is the number of modules in the string and m is the number of modules per segment. If this system is to be scaled, then a cluster of m modules have to be connected together. Similar to previous architectures, the string voltage is the sum of the PV voltages, which presents the same challenge of needing to connect extra power electronic interfaces to integrate it with a DC grid. Along with the above discussed drawbacks, the DMPPT schemes addressed in the literature have not considered Non-MPP mode of operation in their systems.

This paper introduces a topology that aims to address the above challenges. The proposed Series Balancing Capacitor (SBC) based module level DMPPT architecture has a string of PV modules along with a series balancing capacitor (SBC) in series with the string. The DC-DC converters connected across the PV modules have their input connected to the SBC, as a result the switches used in these converters have lower voltage ratings. The SBC also has a DC-DC converter connected across it that is used to maintain a particular voltage, given by the difference in the DC Bus voltage and the summation of the PV voltages. When the operating conditions change, the summation of the PV voltage change and accordingly the SBC voltage is adjusted. This way a fixed DC Bus voltage can be maintained without the need of additional stages of power electronic converters and this system can be integrated easily with a DC grid.

The rest of the paper is structured as follows: Section II discusses the power circuit topology and operation of the proposed system. Section III describes the control strategy of both MPP and non-MPP modes of operation. Section IV describes the system parameters and shows the validation of the control scheme by simulation results of the proposed topology obtained from MATLAB/Simulink software. Lastly, Section V concludes the paper.

II. Power Circuit Configuration

The power circuit configuration of the proposed scheme is shown in Fig.1. For the simplicity in demonstration purposes, three modules (having around 30V MPP at STC) are chosen along with a Series Balancing Capacitor (SBC) connected to a 120V DC Microgrid [15]. This scheme can be expanded to any number of modules, depending on the DC grid voltage required. A distributed architecture is adopted wherein each module has a DC-DC converter connected across it that maintains a particular voltage across it to control the module's output power. Flyback converters have been chosen for simplicity, and they can be replaced by a suitable isolated DC-DC converter as per the required power rating.

A. Mathematical Analysis

The following mathematical analysis has been done for 3 modules connected in the string. For ease of explanation, the converters are assumed to be lossless.

A particular scenario has been taken into account where all the modules receive varying illuminations, with Module 1 receiving the highest illumination among the three modules. The string and the PV currents have been considered ripple free at steady state for a given operating condition.

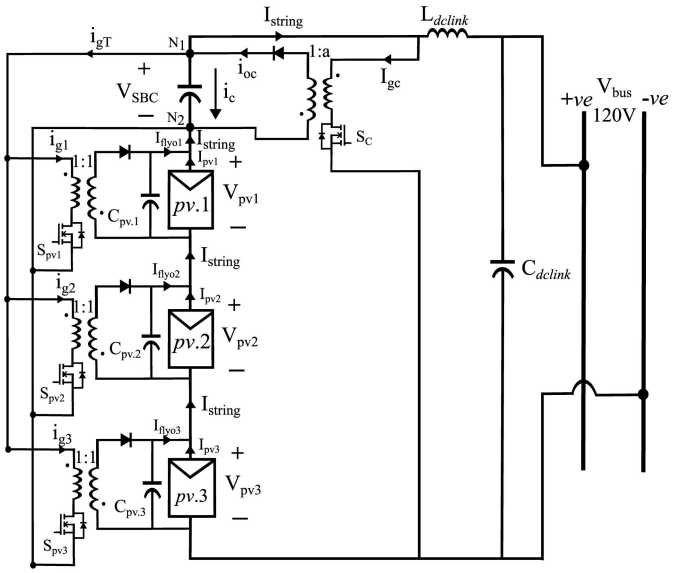

Fig. 1. Circuit Diagram for SBC based Module Level DMPPT scheme

The current in the string will be equal to the maximum current of all the three modules, which in this case is I_{pv1},

$$I_{string} = I_{pv1} \tag{1}$$

As a result the output current of Flyback converter 1 is going to be equal to

$$I_{flyo1} = I_{string} - I_{pv1} = 0 \tag{2}$$

Since, the PV currents of the other modules are lower than the string current, the output currents of Flyback converter 2 and 3 are

$$I_{flyo2} = I_{string} - I_{pv2} \tag{3}$$

$$I_{flyo3} = I_{string} - I_{pv3} \tag{4}$$

From this, the individual PV Flyback converter power outputs can be written as

$$P_{flyo1} = V_{pv1} \times I_{flyo1} = 0 \tag{5}$$

$$P_{flyo2} = V_{pv2} \times I_{flyo2} = V_{pv2} \times (I_{string} - I_{pv2}) \tag{6}$$

$$P_{flyo3} = V_{pv3} \times I_{flyo3} = V_{pv3} \times (I_{string} - I_{pv3}) \tag{7}$$

KCL applied at node N1 of SBC Flyback converter gives

$$i_{oc} = i_{gT} + i_c + i_{string} \tag{8}$$

where

i_{oc} = Instantaneous output current of SBC DC-DC converter

i_c = Instantaneous SBC current
$i_{gT} = \sum_{i=1}^{3} i_{gi}$ = Sum of the PV Flyback converter input currents

Since the average current through the SBC will be 0, the average power processed by the SBC DC-DC converter is given by

$$\begin{aligned} P_{flySBC} &= V_{SBC} \times I_{oc} \\ &= V_{SBC} \times (I_{gT} + I_{string}) \\ &= V_{SBC} \times ((I_{g1} + I_{g2} + I_{g3}) + I_{string}) \end{aligned} \tag{9}$$

where, V_{SBC} = V_{bus} - $(\sum_{i=1}^{3} V_{pvi})$

Assuming the efficiency of the PV Flyback converters to be 100%, the input power of the PV Flyback converters is going to be equal to the output power.

Hence,

$$\begin{aligned} V_{SBC} \times I_{g1} &= V_{pv1} \times I_{flyo1} = P_{flyo1} \\ V_{SBC} \times I_{g2} &= V_{pv2} \times I_{flyo2} = P_{flyo2} \\ V_{SBC} \times I_{g3} &= V_{pv3} \times I_{flyo3} = P_{flyo3} \end{aligned} \tag{10}$$

Using (9) and (10)

$$P_{flySBC} = P_{flyo1} + P_{flyo2} + P_{flyo3} + (V_{SBC} \times I_{string}) \tag{11}$$

In an extreme scenario of the case considered in equation (2), where only PV module 1 is at STC and the other two modules are severely shaded and generating negligible power, the SBC DC-DC converter has to process nearly the full MPP power of the two shaded modules and maintain the string current which is equal to the MPP current at STC.
In such a case, the PV module and the PV Flyback output currents will be

$$I_{pv1} = I_{mpp} = I_{string}; \quad I_{pv2} \approx 0; \quad I_{pv3} \approx 0 \tag{12}$$

$$I_{flyo1} = 0; \quad I_{flyo2} \approx I_{pv1}; \quad I_{flyo3} \approx I_{pv1} \tag{13}$$

From (12) and (13), the PV module powers and the PV Flyback output powers can be written as (while writing the below equations, the MPP voltages of the PV modules have been approximately taken to be equal under different operating conditions)

$$\begin{aligned} P_{pv1} &= V_{pv1} \times I_{pv1} = V_{mpp} \times I_{mpp} = P_{mpp} \\ P_{pv2} &= V_{pv2} \times I_{pv2} \approx 0; \;\; P_{pv3} = V_{pv3} \times I_{pv3} \approx 0 \\ P_{flyo1} &= V_{pv1} \times I_{flyo1} = V_{pv1} \times (I_{string} - I_{pv1}) = 0 \\ P_{flyo2} &= V_{pv2} \times I_{flyo2} \approx V_{pv2} \times I_{pv1} \approx P_{mpp} \\ P_{flyo3} &= V_{pv3} \times I_{flyo3} \approx V_{pv2} \times I_{pv1} \approx P_{mpp} \end{aligned} \tag{14}$$

where P_{mpp} = PV module output power at STC

Hence, using (11) and (14), the maximum power processed by the SBC DC-DC converter can be calculated as

$$\begin{aligned} P_{flySBC} &= P_{flyo1} + P_{flyo2} + P_{flyo3} + (V_{SBC} \times I_{string}) \\ &\approx 0 + P_{mpp} + P_{mpp} + (V_{SBC} \times I_{mpp}) \\ &\approx 2 \times P_{mpp} + (V_{SBC} \times I_{mpp}) \end{aligned} \tag{15}$$

Equations (11) to (15) can be written for n number of PV modules in a string and using a modified version of equation (15) [shown in (16)], the power rating of the SBC DC-DC converter can be calculated as follows,

$$P_{flySBC} \approx (n-1) \times P_{mpp} + (V_{SBC} \times I_{pvmax}) \tag{16}$$

where, $V_{SBC} = V_{bus} - (\sum_{i=1}^{n} V_{pvi})$
and, I_{pvmax}= MPP current of a PV module STC

Equation (16) shows that the SBC DC-DC converter should have a significantly higher rating compared to PV DC-DC converters, hence a different topology of isolated converters is required. However, for simulation purposes shown in section IV, a Flyback converter is used.

III. Control Structure

A. Control Philosophy

To control any PV module's output power, the voltage across it should be controlled. This is done with the help of DC-DC converters, in this case Flyback converters. The system presented in this paper has two operating modes - MPP mode and Non-MPP mode. In the MPP mode, as the name suggests, the PV modules are going to generate the maximum power according to their respective operating conditions. In Non-MPP mode, the string of PV modules will be made to output a desired amount of power, which will be less than maximum power.
In both of the modes of operation, the individual PV module voltages and currents need to be measured. Along with this, the voltage across the SBC and DC Bus also needs to be measured. Hence, the sensor count required for this system will be $m + 2$ voltage sensors and m current sensors, where m denotes the count of PV modules in the string.
The Flyback converters of the PV modules and the SBC are operated in Discontinuous Conduction Mode (DCM) to achieve improved stability for closed loop control and lower size of the magnetic elements.

B. Realisation of Control Algorithm

1) MPP Mode: In MPP mode of operation, the PV modules will be made to operate at their respective MPP voltages that depend on their present operating conditions. The voltage and the current information of the PV module are measured by the sensors and fed to the MPPT controller that generates a voltage reference (V^*_{pvi}), as shown in Fig. 2(a), and the Flyback converter connected across it operates the PV module at that voltage using a closed loop system. Perturb and Observe

(P&O) is chosen as the MPPT algorithm for this system due to it's inherent simplicity and ease of implementation as stated in [16].

According to the PV module's operating conditions, the reference voltage keeps updating and the balance voltage is adjusted by the SBC as shown in the control diagram of Fig. 2(b).

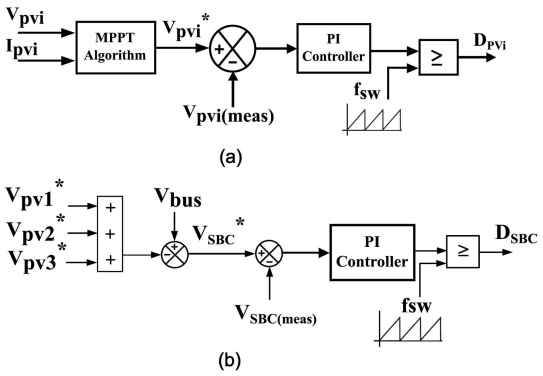

Fig. 2. Control diagram for PV module and SBC Flyback converters

2) Non-MPP Mode: While operating in MPP mode, a situation may arise when the load demand has reduced or some maintenance needs to be carried out on any part of the system. In such a case, a supervisory controller commands the system to shift to Non-MPP mode and also gives information on the power demand to be matched. Before commencing Non-MPP mode, the system was already in MPP mode, and the PV voltages were being controlled at their respective MPP point. Once Non-MPP command is activated by the supervisory controller, the generated power P_{gen}, which is the summation of PV module powers, and the demand power P_{dem} are compared. If P_{gen}>P_{dem}, the voltage reference of all the PV modules are given a positive step change, such that the operating point of the modules shift towards the right hand side of the MPP in the Power-Voltage curve of a PV module as shown in Fig. 3(a). This results in the overall PV power to reduce. This new generated power is again compared with P_{dem} and this process is continued till P_{gen}=P_{dem}. Once this condition is satisfied, that is $\sum_{k=1}^{3} P_{pvk} = P_{dem}$, the voltage references are fixed at that value.

The right hand side of MPP is chosen as the operating region for Non-MPP mode is to limit the voltage rise across the SBC. If the PV modules were operated in the left hand side of the MPP point, the overall PV voltage would have reduce thereby leading to the increment in the voltage across the SBC as per (17). As a consequence, the voltage stress of the SBC may become high if the demanded power is too low.

However, operating the PV modules in the right hand side of MPP poses a problem: if the power demand is too low, the PV modules would need to operate at voltages closer to their open circuit voltage (V_{oc}) and this will cause the SBC voltage to be too low which might compromise the operation of the PV Flyback converters. Hence, to make sure that the SBC voltage never goes below a certain point, the PV powers

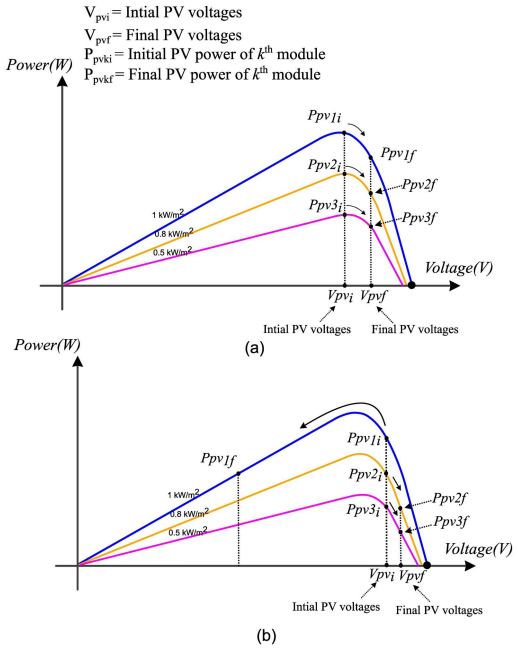

Fig. 3. Operating point of the PV modules in Non-MPP mode

and currents are monitored and just as the SBC voltage crosses the minimum threshold V_{SBCmin}, the voltage of the highest irradiated module is decreased by implementing a negative step change in each cycle, while the voltages of the other two modules continue to increase as before. As a result, the voltage across the SBC slowly starts rising according to equation (17) as well as the overall generated power first increases (till it reaches MPP) and then reduces (left side of MPP). This process is continued till the P_{gen} and P_{dem} are equal. Once they are equal, the PV voltages are fixed at those values, as shown in Fig. 3(b), until the power demand changes.

$$V_{SBC} = V_{bus} - (\sum_{i=1}^{3} V_{pvi}) \tag{17}$$

The operation of Non-MPP mode is explained in the simplified flowchart given in Fig. 4. The flowchart has been made assuming that the system is in MPP mode before being switched to Non-MPP mode.

IV. Simulated Performance

To validate the presented architecture, the power circuit shown in Fig. 1 is simulated in MALTAB/Simulink software. The PV module electrical characteristics for the simulation study are taken according to the characteristics of Vikram-Solar ELDORA VSP.60.AAA.03. The electrical specifications of this module under Standard Test Conditions (STC) are detailed in Table I. As previously stated, the PV and the SBC Flyback converters are operated in discontinuous conduction mode (DCM) by choosing appropriate values of the magnetic elements.

The three modules are considered to be experiencing different insolation levels, although the temperature is kept at 25°C

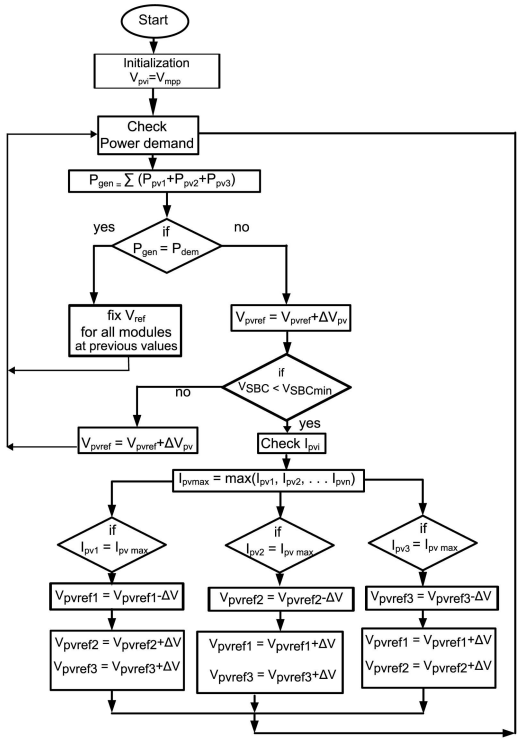

Fig. 4. Flowchart showing the operation of the system in Non-MPP mode of operation

TABLE I
ELECTRICAL DATA OF ELDORA VSP.60.AAA.03 MODULE AT STC

Parameters	*Value*
P_{mpp}	$250W$
Voltage at P_{mpp}, V_{mpp}	$30.6V$
Current at P_{mpp}, I_{mpp}	$8.18A$
Open circuit voltage, V_{oc}	$37.5V$
Short circuit current, I_{sc}	$8.7A$

for all the modules. The electrical data of the modules with the insolation levels considered in the simulations have been shown in Table II.

At STC the given system is supposed to generate 750W of power, however, for the set insolation levels given in Table II, at 25°C the system power reduces to 577W at MPP.

For the simulations, an additional variable has been considered called $Mode$. This variable switches the system from MPP to Non-MPP mode and vice versa. When $Mode$ = 1, system is in MPP mode and when $Mode$ = 0, system is in Non-MPP mode.

TABLE II
ELECTRICAL DATA OF PV MODULES FOR DEFINED INSOLATION LEVELS

Module	*Insolation*	*Voltage at MPP*	*Power at MPP*
Module 1	1 kW/m^2	$30.6V$	$250\ W$
Module 2	0.8 kW/m^2	$30.75V$	$201\ W$
Module 3	0.5 kW/m^2	$30.75V$	$126\ W$
		$\sum = 92.1V$	$\sum = 577\ W$

The system parameters considered for the simulation purposes are stated in Table III. In Fig. 5(a), the $Mode$ signal has been shown. It can be observed that when the $Mode$ signal is set to 1, the system is in MPP mode and is generating 577W of power. At MPP mode, the summation of the PV voltages ($\sum_{i=1}^{3} V_{pvi}$) is about 92V, hence the voltage across the SBC is (120 - 92)V = 28V.

TABLE III
PARAMETERS CONSIDERED FOR SIMULATION STUDY

Parameters	*Value*
DC Bus Voltage, V_{bus}	$120V$
SBC, C_{SBC}	$200\mu F$
Magnetizing inductance of PV Flyback	$2.73\mu H$
Magnetizing inductance of SBC Flyback	$14.5\mu H$
Input voltage range of PV Flyback	20-39V
Output voltage range of PV Flyback	0-37.5V
Input voltage of SBC Flyback	$120V$
Output voltage range of SBC Flyback	20-39V
Switching frequency	$100kHz$

When the $Mode$ signal is shifted to 0, the system switches to Non-MPP mode. In this mode, the system no longer generates maximum power, but tries to match the demand power P_{dem} that can be observed by the blue line in Fig. 5(b). In the simulation, P_{dem} has been considered to be 250W. Once the system enters Non-MPP mode, the voltage references of all the modules begin increasing as seen in Fig. 5(c), and the individual PV power start reducing as seen in Fig. 5(e), as a result the overall power reduces. This goes on until the voltage across the SBC is above V_{SBCmin} that has been taken as 20V. As soon as the SBC voltage V_{SBC} touches 20V, the algorithm changes. In order to keep the V_{SBC} above 20V and satisfy the power demand, the voltage of the module generating maximum current starts reducing, while the voltages of the other two modules are kept on increasing, just as before. This way, V_{SBC} starts increasing above V_{SBCmin} (Fig. 5(d)) and the power keeps on reducing till it reaches P_{dem} of 250W.

For this particular case, when P_{gen} reaches P_{dem}, the steady state PV voltages are 15V, 36V and 36V respectively, while the voltage of the SBC is around 33V. The SBC was chosen such that the maximum voltage ripple across it is 0.78V under ideal conditions, although this may sometimes be exceeded since the SBC ESR also has been taken into account in the simulations.

Taking into consideration the oscillations of the PV voltages and PV powers, a power band of 5W has been considered when comparing P_{gen} and P_{dem}. Similarly, a voltage band of 2V is taken for V_{SBC}.

The $Mode$ signal has been shifted to 1 again after some time to show that the system successfully tracks the MPP power of 577W as per the set insolation levels mentioned in Table II.

V. CONCLUSION

This paper introduces a Distributed Maximum Power Point Tracking (DMPPT) scheme designed to extract the maximum power from a string of PV modules under mismatched conditions. This architecture will have a wide array of applications

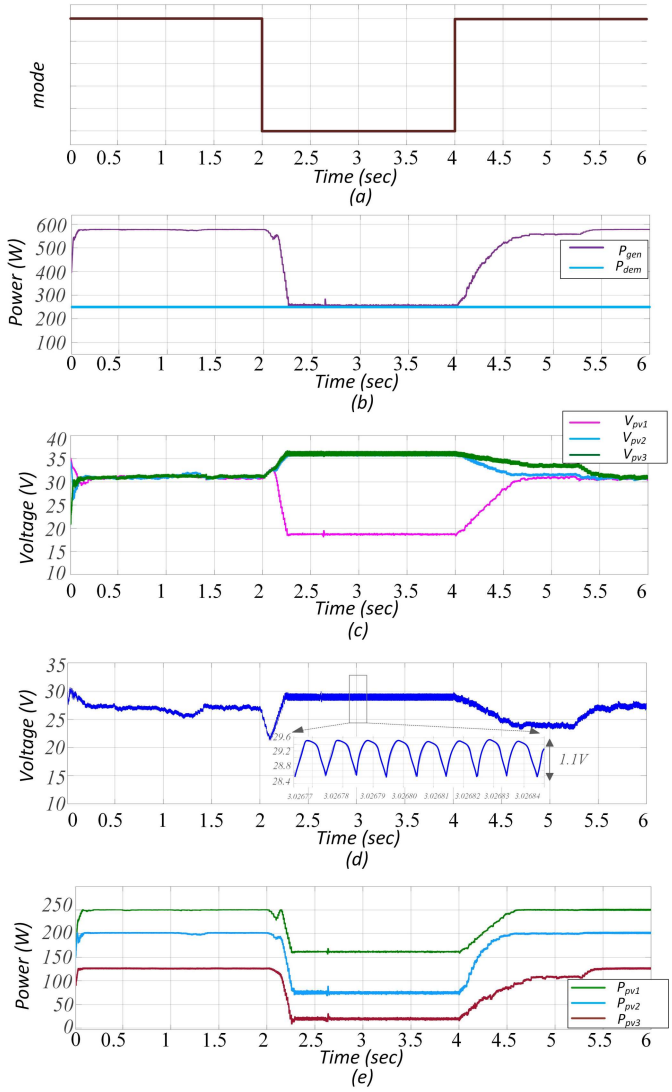

Fig. 5. Simulated performance of the system - (a) Mode signal, (b) Generated Power(P_{gen}) and Demanded Power (P_{dem}), (c) PV module voltages, (d) SBC Voltage, (e) PV module Powers

in urban infrastructure where the PV systems need integration with a DC grid, especially in BIPV applications. The advantages of this scheme are - (i) no full power processing power electronic interfaces required to get a desired DC voltage, (ii) PV modules can operate at their MPPs and maintain a fixed DC Bus voltage, (iii) MPP and Non-MPP mode functionality, (iv) lower switch voltage ratings of the PV DC-DC converters, and (iv) easy scalability and modularity. The control issues of this architecture, especially in Non-MPP mode are discussed and the validation of this scheme has been proved by detailed simulation study.

VI. Acknowledgment

This work was supported by the Department of Science and Technology funded by SERB Centre of Energy Transformation and Storage for the project titled “Centre of Excellence on Energy Aware Urban Infrastructure”, Government of India.

References

[1] T. Shimizu, M. Hirakata, T. Kamezawa and H. Watanabe, “Generation control circuit for photovoltaic modules,” in IEEE Transactions on Power Electronics, vol. 16, no. 3, pp. 293-300, May 2001.

[2] H. Jeong, H. Lee, Y. -C. Liu and K. A. Kim, “Review of Differential Power Processing Converter Techniques for Photovoltaic Applications,” in IEEE Transactions on Energy Conversion, vol. 34, no. 1, pp. 351-360, March 2019.

[3] C. Olalla, D. Clement, M. Rodriguez and D. Maksimovic, “Architectures and Control of Submodule Integrated DC–DC Converters for Photovoltaic Applications,” in IEEE Transactions on Power Electronics, vol. 28, no. 6, pp. 2980-2997, June 2013.

[4] S. Poshtkouhi, J. Varley, R. Popuri and O. Trescases, “Analysis of distributed peak power tracking in photovoltaic systems,” The 2010 International Power Electronics Conference - ECCE ASIA -, Sapporo, Japan, 2010, pp. 942-947.

[5] P. S. Shenoy, K. A. Kim, B. B. Johnson and P. T. Krein, “Differential Power Processing for Increased Energy Production and Reliability of Photovoltaic Systems,” in IEEE Transactions on Power Electronics, vol. 28, no. 6, pp. 2968-2979, June 2013.

[6] Aniruddha K. M., J. Biswas, Anjana K. G., M. Barai, “A Simple Real-Time DMPPT Algorithm for PV Systems Operating under Mismatch Conditions,” in Journal of Power Electronics, vol 18, no. 3, pp. 826-840, May 2018.

[7] D. Debnath, P. De, K. Chatterjee, “Simple scheme to extract maximum powerfrom series connected photovoltaic modulesexperiencing mismatched operatingconditions,” IET Power Electronics, Vol. 9, No. 3, pp. 408-416, Mar. 2016.

[8] S. N. Ghosh and D. Debnath, “An Approach to Reduce the Number of Sensors for MPPT of Series Connected Solar PV Modules Facing Mismatched Operating Conditions,” 2018 8th IEEE India International Conference on Power Electronics (IICPE), Jaipur, India, 2018, pp. 1-6.

[9] X. Wang et al., “Performance Quantization and Comparative Assessment of Voltage Equalizers in Mismatched Photovoltaic Differential Power Processing Systems,” in IEEE Transactions on Power Electronics, vol. 39, no. 1, pp. 1656-1675, Jan 2024.

[10] R. C. N. Pilawa-Podgurski and D. J. Perreault, “Submodule Integrated Distributed Maximum Power Point Tracking for Solar Photovoltaic Applications,” in IEEE Transactions on Power Electronics, vol. 28, no. 6, pp. 2957-2967, June 2013.

[11] L. Lin, J. Zhang and S. Shao, “Differential Power Processing Architecture With Virtual Port Connected in Series and MPPT in Submodule Level,” in IEEE Access, vol. 8, pp. 137897-137909, 2020.

[12] A. D. Grasso, S. Pennisi, M. Ragusa, G. M. Tina, C. Ventura, “Performance evaluation of a multistringphotovoltaic module with distributed DC–DC converters” Cover Image IET Renewable Power Generation, Issue 8, Vol. 9, No. 3, pp. 408-416, Mar. 2016.

[13] Tao Zhang, Jiahui Jiang, Daolian Chen, “An efficient and low-cost DMPPT approach for photovoltaic submodule based on multi-port DC converter”, Renewable Energy, Volume 178,2021, Pages 1144-1155.

[14] H. Jeong, S. Park, J. -H. Jung, T. Kim, A. -R. Kim and K. A. Kim, “Segmented Differential Power Processing Converter Unit and Control Algorithm for Photovoltaic Systems,” in IEEE Transactions on Power Electronics, vol. 36, no. 7, pp. 7797-7809, July 2021.

[15] S. Anand and B. G. Fernandes, “Optimal voltage level for DC microgrids,” IECON 2010 - 36th Annual Conference on IEEE Industrial Electronics Society, Glendale, AZ, USA, 2010.

[16] R. B. Bollipo, S. Mikkili and P. K. Bonthagorla, “Hybrid, optimal, intelligent and classical PV MPPT techniques: A review,” in CSEE Journal of Power and Energy Systems, vol. 7, no. 1, pp. 9-33, Jan. 2021.